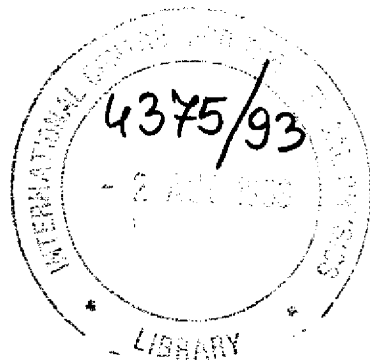

IC/93/153

INTERNATIONAL CENTRE FOR
THEORETICAL PHYSICS

AB-INITIO CALCULATION OF THE VALENCE-BAND OFFSET AT STRAINED GaAs/InAs (001) HETEROJUNCTION

Nacir Tit

Maria Peressi

and

Stefano Baroni

INTERNATIONAL
ATOMIC ENERGY
AGENCY

UNITED NATIONS
EDUCATIONAL,
SCIENTIFIC
AND CULTURAL
ORGANIZATION

MIRAMARE-TRIESTE

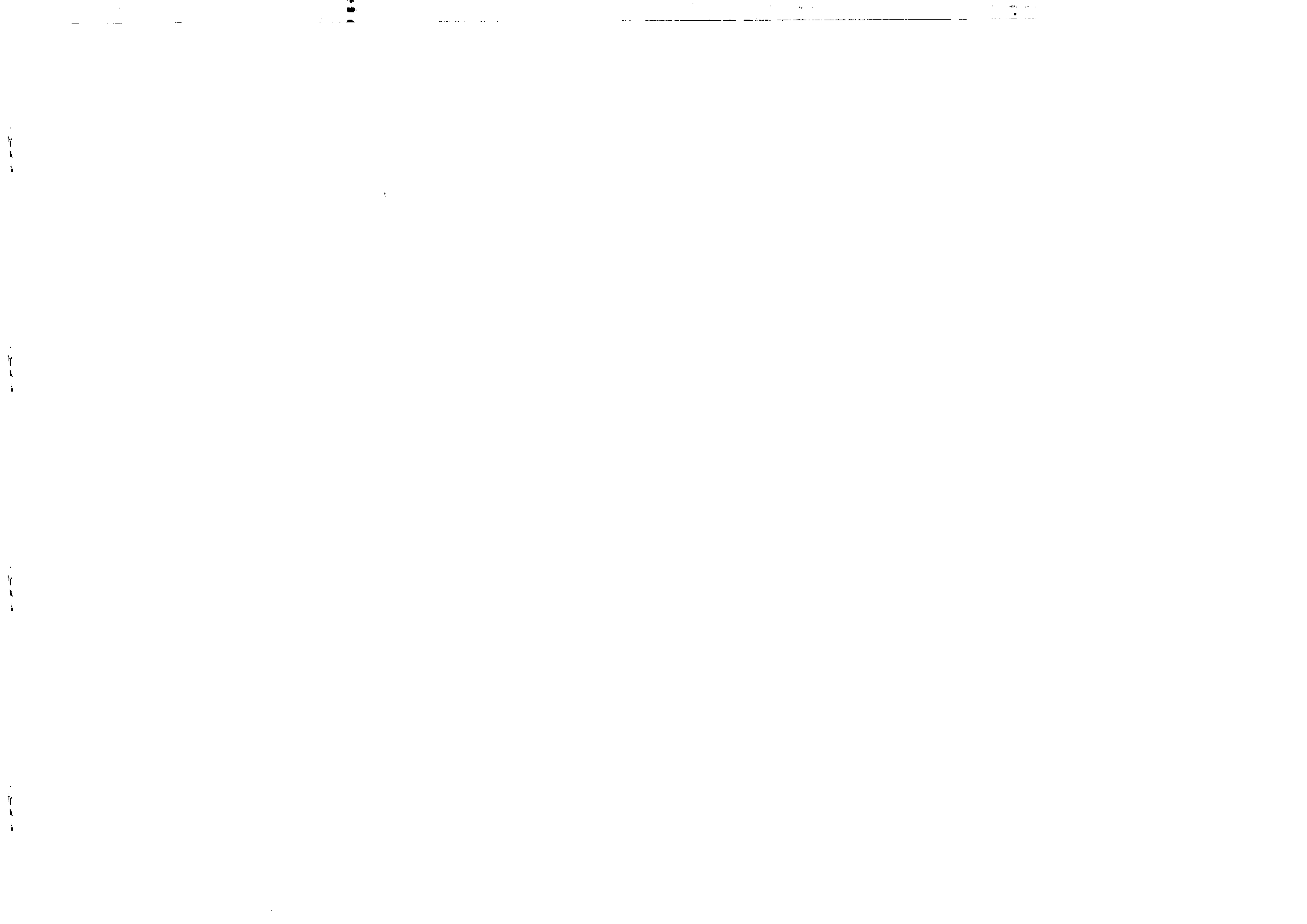

IC/93/153

International Atomic Energy Agency
and
United Nations Educational Scientific and Cultural Organization
INTERNATIONAL CENTRE FOR THEORETICAL PHYSICS

AB-INITIO CALCULATION OF THE VALENCE-BAND OFFSET AT STRAINED GaAs/InAs (001) HETEROJUNCTION

Nacir Tit
International Centre for Theoretical Physics, Trieste, Italy,

Maria Peressi
Dipartimento di Fisica Teorica dell'Università di Trieste, Trieste, Italy

and

Stefano Baroni
Scuola Internazionale Superiore di Studi Avanzati (SISSA), Trieste, Italy.

ABSTRACT

We present a self consistent pseudopotential calculation of the valence band offset (VBO) at GaAs/InAs (001) strained heterojunction, which is chosen as an example of the isovalent polar with common anion lattice mismatched heterojunctions. The effects of strain are studied by looking at the variation of the VBO versus the in plane lattice constant, which is imposed by the substrate. Our results show that the VBO can be tuned by about 0.17 eV going from GaAs to InAs substrates. Comparison of our work with the available experimental and theoretical results is also discussed.

MIRAMARE – TRIESTE
June 1993

1 Introduction

Band discontinuities at semiconductor heterojunctions[1] are important parameters controlling the transport properties in nanostructure devices. It is of great interest for both fundamental and applied research to understand the factors and mechanisms restraining the band offsets.[2] A lot of experimental as well as theoretical work has been already done for lattice-matched heterojunctions. From the theoretical point of view, in particular, several different approaches – even model theories[3] – have been successful in determining correctly the band offset at a large class of systems (namely *isovalent* junctions), where they are found to be independent of the interface details.[2] For the lattice-mismatched case, conversely, the field is still open and little theoretical work has been done. From the experimental point of view, difficulties arise not only for the determination of the valence band offset (VBO), but even for the growth of the pseudomorphic epilayer, that should be restricted to very few layers so that to avoid misfit dislocations.

Recently, there have been some interests in GaAs/InAs superlattices because of their applications in high-speed and optoelectronic devices. Despite of their importance, only a few experiments determining the VBO have been reported in the literature for such system. It has about 7% of lattice mismatch and the critical thickness for dislocation generation is as thin as 2 monolayers. Kowalczyk and co-workers[4] reported a measurement of the VBO, in the InAs/GaAs (001) heterojunction grown on GaAs substrate, using x-ray photoemission spectroscopy (XPS). They found a VBO value of about 0.17 ± 0.07 eV. However the thickness of the InAs overlayer in their sample is about $20\AA$, which is much bigger than the critical value for dislocation generation. Therefore, it is believed that their VBO value does not correspond to the VBO existing at a defect-free interface in pseudomorphic heterojunction. In a more recent XPS measurements, reported by Hirakawa

et al.[5], more careful considerations have been taken about the overlayer thickness. They have used two different samples: InAs layer pseudomorphically grown on GaAs substrate (type I) and GaAs layer grown on InAs substrate (type II). Their band offsets measured between the averages of top valence-band manifold states were VBO_{ave}= 0.27eV for type I and 0.36eV for type II (InAs region higher). The authors also reported the VBO of 0.53eV and -0.16eV, for the previous type I and type II respectively, as referred from the GaAs top valence band. A much larger band offsets have been predicted by Menéndez et al.[6] (VBO_{ave} = 0.49 ± 0.1 eV for type I) through an extrapolation of the value obtained using the scattering experiment on $In_{0.05}Ga_{0.95}$As/GaAs quantum wells.

Interface related effects (such as charge transfer and interface states) might contribute to the band lineups at the strained heterojunction. In this respect, the self-consistent interface calculations[2,7-11] have shown their superiority over the model theories. Cardona and Christensen[12] predicted VBO= 0.52 eV for type I, using the dielectric midgap energy theory, which is in excellent agreement with Hirakawa's value (0.53 eV)[5]. However, the determination of the midgap point contains some difficulties and ambiguities.[13] Priester and co-workers[10] obtained VBO_{ave} of a value 0.09 eV for type I and 0.19 eV for type II using the self-consistent tight-binding calculations. More recently, Taguchi and Ohno[11] reported VBO_{ave}= 0.02 eV for type I and 0.01 eV for type II using the ab-initio self-consistent pseudopotential method in the absence of spin-orbit splittings.

This paper is devoted to calculate the VBO at the strained GaAs/InAs (001) heterojunction using the self-consistent pseudopotential supercell method and to investigate the strain effects by varying the substrate (the in-plane lattice constant). We divide the VBO problem into two parts:

$$VBO = \Delta E_v + \Delta V \tag{1}$$

The first term (ΔE_v) is the band structure term, which is an intrinsic bulk property, obtained from two separate standard band-structure calculations for each of the two bulks in the appropriate strained configurations, and ΔE_v is the difference between the energies of the two valence band edges when the average electrostatic potentials are aligned. The second term (ΔV) is the electrostatic potential lineup, which contains interface-specific effects, and can be evaluated only from a supercell calculation. This latter term is generated by both the valence electronic charge distribution and the charge of the bare ion cores. The total electrostatic potential consists of the Hartree, the exchange-correlation and the local part of the ionic potential. More details about the calculation of lineup will be described in section 4.

Our calculations have been performed using the state-of-the-art density functional theory (DFT)[14] in the local density approximation (LDA) and applied in the momentum space formalism.[15] We use a plane wave (PW) basis set up to a kinetic energy cutoff of 20 Ry for the band structure term and 12 Ry for the potential lineup term (i.e.: about 112 plane waves per atom in the calculation of the potential lineup term), norm-conserving nonlocal pseudopotentials,[16] and Ceperely-Alder form[17] for the exchange-correlation potential. Special-point technique[18] has been used to perform the $\vec{k}$-space integrations. We have used the (333) Monkhorst-Pack cubic mesh appropriately folded for various supercells. Convergence tests have been carried out to guarantee the quality of the chosen $\vec{k}$-points.

In the next section, we will describe the atomic-scale structure of some systems studied here, in their equilibrium configurations, as imposed by the substrate. Sections 3 and 4 describe the calculation of the band structure term, ΔE_v, and the potential lineup term, ΔV, respectively. The last section summarizes our results and findings.

2 Determination of the atomic-scale structures

The growth of a perfect pseudomorphic heterostructure is possible only if the epilayer do not exceed certain critical thickness characteristic of the material and dependent on the degree of mismatch. In the case of the pseudomorphic growth, the substrate controls the in-plane lattice constant ($a_{\parallel} = a_{sub.}$). The biaxial strain due to the lattice mismatch make the epilayer expand or compress along the growth direction and accommodate a new inter-plane lattice constant $a_{\perp}$. In the unstrained configurations, the equilibrium lattice parameters calculated with a cutoff of 12 Ry are: a_{GaAs}= 10.63 a.u. and a_{InAs}= 10.25 a.u. These values give a lattice mismatch of 5.7%, which is a little less than the experimental one. The elastic constants[19] have also been calculated and are listed in table 1, where the square brackets contain the experimental data[20] for comparison. It was shown[21] that for many lattice-mismatched heterostructures the equilibrium interplanar spacing can be determined to a good approximation using the macroscopic theory of elasticity, which predicts (for a pure epitaxially strained material grown along the (001) direction) the following:

$$\begin{aligned}
a_{\parallel} &= a_{subs.} = a_{\perp subs.} \\
a_{\perp str.} &= a_{str.}\left[1 - 2\left(\frac{c_{12}}{c_{11}}\right)_{str.}\left(\frac{a_{\parallel}}{a_{str.}} - 1\right)\right] \\
\epsilon_{xx}^{str.} &= \epsilon_{yy}^{str.} = \epsilon_{\parallel str.} = \frac{a_{\parallel}}{a_{str.}} - 1 \\
\epsilon_{zz}^{str.} &= \epsilon_{\perp str.} = \frac{a_{\perp str.}}{a_{str.}} - 1 \qquad (2) \\
Tr\left(\overleftrightarrow{\epsilon}\right) &\approx \frac{\Delta\Omega}{\Omega} \\
\tilde{a}_{str.} &= \left(a_{\parallel}^2 a_{\perp}\right)^{1/3} \approx \left[1 + \frac{1}{3}Tr(\overleftrightarrow{\epsilon})\right] a_{str.}
\end{aligned}$$

where $\overleftrightarrow{\epsilon}$ is the strain tensor, Ω is the equilibrium bulk volume of the material deposited, $\Delta\Omega$ is the change due to the strain, c_{ij} are the elastic constants, the label *subs.* refers to the cubic substrate and *str.* to the strained epilayer. $\tilde{a}_{str.}$ is an effective lattice constant of a cubic material with the same volume of the strained configuration. In table 2 we report the structural parameters for GaAs and InAs grown on different substrates, calculated using the macroscopic theory of elasticity, Eqs.(2), and the theoretical parameters reported in table 1. Three substrates are considered in the study of strain effects on the VBO: (i) InAs epilayer pseudomorphically grown on a GaAs substrate (supercell 1); (ii) Both GaAs and InAs are strained as being grown on $Ga_{0.5}In_{0.5}As$ substrate (supercell 2). The lattice constant (10.98 a.u.) of this substrate was calculated by using the virtual crystal approximation (VCA). This value is very close to the average (10.94 a.u.) between a_{GaAs} and a_{InAs}; (iii) GaAs epilayer grown on an InAs substrate (supercell 3).

Since the macroscopic theory of elasticity cannot predict the interface atomic-scale structure, we calculated the total electrostatic potential lineup (see section 4) using the supercell 1 with various atomic configurations, which were obtained by moving the interfacial As-atomic plane in the z-direction (from -0.0016 $a_{\parallel}$ to 0.0016 $a_{\parallel}$ around the initial As plan position, as predicted by the macroscopic theory of elasticity). We found that this has a negligible effect on the band lineup within our numerical accuracy (which is estimated to 40 meV). This problem of interface effects will be discussed further in section 4. Throughout the rest of this paper only perfect heterojunctions are considered.

3 Band structure term

In the three supercells considered here, the composants InAs and GaAs are in different strain conditions. It is known that each of these two materials possesses a direct bandgap at Γ-point regardless of the strain state.[22] Neglecting the spin-orbit splittings, which will be added in a *posteriori*, we performed a self-consistent pseudopotential calculation on each strained or unstrained configuration using a kinetic energy cutoff of 20 Ry to evaluate the valence band eigen-energies at the Γ-point.[2] When a uniaxial strain is introduced in the (001) direction, the crystal point-group symmetry changes from T_d into D_{2d}. This symmetry reduction causes the 3-fold topmost valence-band states to split into 2 degenerate states and one-fold state separated by an energy gap of $\frac{3}{2}\delta E_{001}$. In the uniaxially expanded (biaxially compressed) InAs, the one-fold state is lower in energy; but in the uniaxially compressed (biaxially expanded) GaAs, this state is higher in energy. The corresponding energies for each of these three states of GaAs and InAs are shown in Fig.1a1 and Fig.1.a2 respectively (together with their average —solid line—) versus the in-plane lattice constants in absence of spin-orbit coupling effects. The dotted line corresponds to the one-fold state. Taking into account also the spin degeneracy, the valence-band top edge at Γ-point which includes six states would be divided into a quadruplet and a doublet (which is called the spin-off (so) state) separated by en energy Δ_o because of the spin-orbit interaction. Moving away from the Γ point, the quadruplet is further split into 2 doublets, light-hole (lh) and heavy-hole (hh).

The top of the valence band of zinc blend (or diamond) structure is located at the Γ-point. Neglecting the spin degeneracy, it contains 3 states which are degenerate at Γ-point in the absence of strain effects. In case of the combined effects of strain and spin-orbit coupling, the following shifts are calculated with respect to the average ($E_{v,av}$) of the valence-band top-edge manifolds:

$$
\begin{aligned}
\Delta E_{v,hh} &= +\frac{1}{3}\Delta_o - \frac{1}{2}\delta E_{001}, \\
\Delta E_{v,lh} &= -\frac{1}{6}\Delta_o + \frac{1}{4}\delta E_{001} + \frac{1}{2}\left[\Delta_o^2 + \Delta_o \delta E_{001} + \frac{9}{4}\left(\delta E_{001}\right)^2\right]^{1/2}, \quad (3) \\
\Delta E_{v,so} &= -\frac{1}{6}\Delta_o + \frac{1}{4}\delta E_{001} - \frac{1}{2}\left[\Delta_o^2 + \Delta_o \delta E_{001} + \frac{9}{4}\left(\delta E_{001}\right)^2\right]^{1/2}.
\end{aligned}
$$

The inclusion of the spin-orbit effect in our band structure calculation is done a *posteriori* using the experimental data[20] (Δ_o= 0.34 eV for GaAs and 0.38 eV for InAs). The values of δE_{001} are extracted from our calculations on the strained 4-atom tetragonal cells. We emphasize that δE_{001} is positive in case of uniaxially compressed cell (such as the strained GaAs on InAs substrate) and is negative in case of uniaxially expanded cell (such as the strained InAs on GaAs substrate).

In table 3, we report the values of $E_{v,av}$ and δE_{001} obtained from our standard band-structure calculations using a kinetic energy cutoff of 20 Ry. In these calculations, cubic cells containing 2 atoms and tetragonal cells containing 4 atoms have been used to represent the unstrained and strained configurations respectively. We summarize our results, after the inclusion of spin-orbit interaction, for the GaAs in Fig.1.b1 and for the InAs in Fig.1.b2. In all figures 1 the solid line corresponds to the weighted average ($E_{v,av}$) of the split manifolds; the dotted and the dashed lines to the split states. One can see in Fig.1 that the variation $\Delta E_{v,av}$ is very small ($\approx$ 0.05eV) when the substrate changes from GaAs to InAs. However the difference between the topmost states $\Delta E^{rel.}_{v,top}$ is very sensitive to the effects of bulk "macroscopic" strain, and is changing by about 0.4eV between the two extreme stress configurations. The latter consists of the first term of the right hand side of Eq.(1). To get information about band discontinuities, we still have to perform the potential lineup (ΔV) calculation, which will be described in

the next section.

4 Potential lineup term

Self-consistent calculations have been performed on three different pseudomorphic $(GaAs)_3/(InAs)_3$ (001) supercells constrained to different substrates as described in section 2. In this type of calculation we used a kinetic energy cutoff of 12 Ry. Figures 2a and 2b display the contour plots of the valence electronic density in the (110) and (100) planes respectively in case of supercell 1. The atomic positions are also indicated. Since the electron density $n(\vec{r})$ and the electrostatic potential $V(\vec{r})$ are periodic in the planes nominal to the growth direction (z-axis) and since we are interested in their z-dependence, we show in figure 2c (solid line) the (xy) planar average of the electron density $\overline{n}(z)$. The density is normalized to eight electrons per unit cell. Moreover, in order to get rid of the microscopic bulk oscillations and to blow up the interface features, we apply to $\overline{n}(z)$ (the solid curve in Fig.2c) the double macroscopic average procedure described in reference 8a, to get $\overline{\overline{n}}(z)$ (the dotted curve in Fig.2c). The latter curve reflects the effectiveness of the macroscopic averaging and also that our supercell is long enough to recover the bulk feature at midway between the two interfaces. Then we solved the one-dimensional (1D) Poisson equation using the charge density $\overline{\overline{n}}(z)$ to obtain the electronic potential. Similarly, we calculated the electrostatic potential generated by the bare ionic cores. Figure 2d shows the total (electronic plus ionic) electrostatic potential, $\overline{\overline{V}}(z)$, whose difference between the values in InAs and GaAs regions gives the potential lineup ΔV. A similar calculation has been performed at lower energy cutoff of 8 Ry to assess the convergence of ΔV. We found that the difference is within our numerical accuracy. The 12 Ry energy cutoff is chosen, however, because it describes the bulk properties better.

5 Discussion and conclusions

The previous calculations, presented in sections 3 and 4, have been repeated for the supercells 2 and 3 whose substrates are $Ga_{0.5}In_{0.5}As$ and InAs respectively. Figure 3 presents the results of electrostatic potentials $\overline{\overline{V}}(z)$ for all the 3 supercells. We emphasize that the three supercells do have different lengths, but the corresponding figures are differently scaled in z-direction in order to be shown on the same panel. In table 4 the values of lineups ΔV are listed (where the InAs region is higher in energy). It, also, shows the values of VBO, $\Delta E^{rel.}_{v,top} + \Delta V$, referred from the top of GaAs valence band. The same table contains the values of VBO_{ave}, $\Delta E_{v,av} + \Delta V$, referred from the GaAs region. It is noticeable that the variation of the latter kind of VBO is small with respect to the substrate. This is consistent with the findings of Ref.8a, that reports a study of the isovalent nonpolar lattice-mismatched Si/Ge system. In contrast to the latter system and the heterovalent polar lattice-mismatched Si/GaAs system,[23] our potential lineup is found to be not very sensitive to fine relaxations (with respect to the predictions of the macroscopic theory of elasticity) of the atomic positions at the interface. In table 5, we list our results of the VBO and the VBO_{ave} and compare them to the available theoretical and experimental data. To some extent, our results agree with the XPS experiment of Kowalczyk and co-workers,[4] and, Taguchi and Ohno's pseudopotential calculations.[11] Inevitably, this table obviously calls for deeper experimental and theoretical analyses.

In a summary, we presented a self-consistent pseudopotential calculation of the VBO at the strained GaAs/InAs (001) heterojunctions. We have shown that the strain can tune the VBO up to 0.47eV by varying the substrate from GaAs to InAs. However the VBO as measured between the valence band top manifolds averages is not very sensitive to the interface strain as compared to our numerical accuracy. The conclusion is that the

VBO in such isovalent polar with common-anion lattice mismatched heterojunction is a bulk property because it is quite sensitive to the macroscopic strain (namely bandgap engineering). As far as the theoretical side is concerned, the effects of interface details (such as orientation, abruptness and relaxation) and states are under investigation.

Acknowledgments

One of us (N.T.) thanks A. Dal Corso for a stimulating discussion, the ICTP computer section for their support, and Prof. Abdus Salam, the International Atomic Energy Agency and the UNESCO for their hospitality at the International Center for Theoretical Physics in Trieste.

References

1. F. Capasso and G. Margaritondo, "Heterojunction band discontinuities: Physics and device application", (North-Holland, Amsterdam, 1987); G. Margaritondo, "Electronic structure of semiconductor heterojunctions", (Jaca Book, Milan, 1988).

2. S. Baroni, R. Resta, A. Baldereschi and M. Peressi, in "Spectroscopy of Semiconductor Microstructures", Eds.: G. Fasol, A. Fasolino and P. Lugli (NATO series, New York, 1989), Vol. 206, 251.

3. (a)- C. G. Van de Walle, Phys. Rev. B **39**, 1871 (1989); (b)- C. G. Van de Walle and R. M. Martin, Phys. Rev. B **35**, 8154 (1987); J. Vac. Sci. Tech. B **4**, 1055 (1986); W. Frensley and H. Kroemer, J. Vac. Sci. Tech. **13**, 810 (1976).

4. S. P. Kowalczyk, W. J. Schaffer, E. A. Kraut and R. W. Grant. J. Vac. Sci. Tech. **20**, 705 (1982).

5. K. Hirakawa, Y. Hashimoto, K. Harada and T. Ikoma, Phys. Rev. B **44**, 1734 (1991).

6. J. Menéndez, A. Pinczuk, D. J. Werder, S. K. Sputz, R. C. Miller, D. L. Sivco and A. Y. Cho, Phys. Rev. B **36**, 8165 (1987).

7. A. Baldereschi, S. Baroni and R. Resta, Phys. Rev. Lett. **61**, 734 (1988); D. M. Bylander and L. Kleinman, Phys. Rev. Lett. **59**, 2091 (1987); S. H. Wei and A. Zunger, Phys. Rev. Lett. **59**, 144 (1987).

8. (a)- L. Colombo, R. Resta and S. Baroni, Phys. Rev. B **44**, 5572 (1991); (b)- M. S. Hybertsen, Mat. Res. Soc. Symp. Proc. **148**, 329 (1989); S. Froyen, D. M. Wood, and A. Zunger, Phys. Rev. B **37**, 6893 (1988); J. E. Bernard and A. Zunger, Phys. Rev. B **44**, 1663 (1991).

9. A. Qteish and R. J. Needs, Phys. Rev. B **42**, 3044 (1990).

10. C. Priester, G. Allan and M. Lannoo, Phys. Rev. B **38**, 9870 (1988).

11. A. Taguchi and T. Ohno, Phys. Rev. B **39**, 7803 (1989).

12. M. Cardona and N. E. Christensen, Phys. Rev. B **35**, 6182 (1987).

13. J. Tersoff, Surf. Sci. **168**, 275 (1986).

14. P. Hohenberg and W. Kohn, Phys. Rev. **136**, B864 (1964); W. Kohn and L.J. Sham, Phys. Rev. **140**, A1133 (1965).

15. J. Ihm, A. Zunger and M. L. Cohen, J. Phys. C **12**, 4409 (1979).

16. The pseudopotentials used here are slightly different [P. Giannozzi, unpublished] from those of Bachelet and co-workers and are designed to better reproduce the lattice mismatch between InAs and GaAs. For a general description see: D. R. Hamann, M. Schlüter and C. Chiang, Phys. Rev. Lett. **43**, 1494 (1979); G. B. Bachelet, D. R. Hamann and M. Schlüter, Phys. Rev. B **26**, 4199 (1982).

17. D. M. Cepereley and B. J. Alder, Phys. Rev. Lett. **45**, 566 (1980); J. Perdew and A. Zunger, Phys. Rev. B **23**, 5048 (1981).

18. A. Baldereschi, Phys. Rev. B. **7**, 5212 (1973); H. J. Monkhorst and J. P. Pack, Phys. Rev. B **13**, 5188 (1976).

19. O. H. Nielsen and R. M. Martin, Phys. Rev. B **32**, 3792 (1985).

20. Landolt-Börnstein, Numerical data and functional relationships in science and technology (Springer, New York, 1982), Vol. 17a.

21. C. G. Van de Walle and R. M. Martin, Phys. Rev. B **34**, 5621 (1986).

22. A. Taguchi and T. Ohno, Phys. Rev. B **36**, 1696 (1987).

23. M. Peressi, L. Colombo, R. Resta, S. Baroni and A. Baldereschi, submitted to Phys. Rev. B

24. J. Tersoff, J. Vac. Sci. Tech. B **3**, 1157 (1985).

25. G. Margaritondo, Phys. Rev. B **31**, 2526 (1985).

Table Captions

Table 1: Equilibrium theoretical lattice and elastic constants calculated for GaAs and InAs with a kinetic energy cutoff of 12 Ry. The square brackets corresponds to experimental data[20].

Table 2: Equilibrium structural parameters for GaAs and InAs, grown pseudomorphically on various substrates, as calculated using both table 1 and the macroscopic theory of elasticity.

Table 3: Valence band parameters for unstrained and strained GaAs and InAs configurations. $E_{v,av}$= the average of the split valence-band top-edge manifolds; δE_{001}= the strain splitting energy parameter. The last rows show the difference of the valence band states in the two materials (GaAs higher), calculated between the average of the manifolds ($\Delta E_{v,av}$) and between the topmost states neglecting ($\Delta E_{v,top}^{non-rel.}$) and including ($\Delta E_{v,top}^{rel.}$) the spin-orbit interaction. All energies are in eV and obtained from calculations with a kinetic energy cutoff of 20 Ry.

Table 4: Electronic potential lineup ΔV and the valence band offsets VBO [$\equiv \Delta E_{v,top}^{rel.} + \Delta V$] and VBO_{ave} [$\equiv \Delta E_{v,av} + \Delta V$] for $GaAs/InAs$ (001) superlattice versus the in-plane lattice constants, which are imposed by various substrates. The averaged electrostatic potential is always higher in InAs region. The zero-energy in the VBO and VBO_{ave} values is set at the GaAs topmost and average manifolds respectively with the inclusion of the potential lineups. The calculations of the potential lineups are performed with a kinetic energy cutoff of 12 Ry.

Table 5: Valence band offsets VBO and VBO_{ave} using various theoretical and experimental techniques for comparison to our results.

Table 1

material	a_o(a.u.)	c_{11}(Mbar)	c_{12}(Mbar)	$2(c_{12}/c_{11})$
GaAs	10.63 [10.68]	1.11 [1.18]	0.41 [0.53]	0.74 [0.90]
InAs	11.25 [11.44]	0.86 [0.83]	0.39 [0.45]	0.91 [1.08]

Table 2

	$a_{\parallel}$(a.u.)	10.63 ($GaAs$ subs.)	10.98 ($Ga_{.5}In_{.5}As$ subs.)	11.25 ($InAs$ subs.)
GaAs	$a_{\perp}$(a.u.)	10.63	10.36	10.16
	$\epsilon_{xx}=\epsilon_{yy}=\epsilon_{\parallel}$	—	+0.034	+0.059
	$\epsilon_{zz}=\epsilon_{\perp}$	—	-0.025	-0.043
	$Tr(\overleftrightarrow{\epsilon}) \approx \frac{\Delta\Omega}{\Omega}$	—	+0.042	+0.074
	$\bar{a}$(a.u.)	10.63	10.77	10.87
InAs	$a_{\perp}$(a.u.)	11.82	11.49	11.25
	$\epsilon_{xx}=\epsilon_{yy}=\epsilon_{\parallel}$	-0.055	-0.024	—
	$\epsilon_{zz}=\epsilon_{\perp}$	+0.050	+0.022	—
	$Tr(\overleftrightarrow{\epsilon}) \approx \frac{\Delta\Omega}{\Omega}$	-0.060	-0.026	—
	$\bar{a}$(a.u.)	11.01	11.15	11.25

Table 3

	$a_{\parallel}$(a.u.)	10.63 ($GaAs$ subs.)	10.98 ($Ga_{.5}In_{.5}As$ subs.)	11.25 ($InAs$ subs.)
GaAs	$E_{v,av}$	4.97	4.55	4.27
	δE_{001}	—	+0.21	+0.33
InAs	$E_{v,av}$	4.71	4.32	4.06
	δE_{001}	-0.46	-0.17	—
	$\Delta E_{v,av}$	0.26	0.23	0.21
	$\Delta E_{v,top}^{non-rel.}$	0.04	0.35	0.54
	$\Delta E_{v,top}^{rel.}$	0.02	0.28	0.45

Table 4

$a_{\parallel}$(a.u.)	ΔV (eV)	VBO (eV)	VBO_{ave} (eV)
10.63	0.30	0.28	0.04
10.98	0.28	0.0	0.05
11.25	0.26	-0.19	0.05

Table 5

Method	*Supercell 1* *(GaAs subs.)*		*Supercell 3* *(InAs subs.)*	
	VBO (eV)	VBO_{ave} (eV)	VBO (eV)	VBO_{ave} (eV)
Self-consistent pseudopotential	0.28[a], 0.31[b]	0.04[a], 0.02[b]	-0.19[a], -0.49[b]	0.05[a], 0.01[b]
Self-consistent tight binding[c]	0.46	0.09	-0.34	0.18
Models	0.20[d], 0.52[e], 0.43[f]	0.18[e], 0.19[f]	-0.30[f]	0.18[e], 0.15[f]
Experiments	0.17[g], 0.53[h], 0.21[i]	0.27[h]	-0.16[h]	0.36[h]

[a] Present work
[b] Reference 11
[c] Reference 10
[d] Reference 24
[e] Reference 12
[f] Reference 3a
[g] Reference 4
[h] Reference 5
[i] Reference 25

Figure Captions

Figure 1: The top valence band states for pure and strained GaAs and InAs structures. The calculations include: (a) only strain effects in (a1): GaAs and (a2): InAs. (b) Both strain and spin-orbit splitting effects are included in (b1): GaAs, and (b2): InAs. In all these figures the solid curve corresponds to the weighted average of the valence-band top-edge manifolds, and the dotted curve to the lh state. In (a1) and (a2) the dashed curve is for the two-fold (hh and so) states, but in (b1) and (b2) the latter two states are split into hh state (dashed curve) and so state (dot-dashed curve).

Figure 2: Results of a calculation for $(GaAs)_3/(InAs)_3$ superlattice, grown upon GaAs-substrate. (a) Contour plot of the electronic density in the (110) plane. Atomic positions are indicated. (b) Same as (a) but in the (100) plane. (c) Planar averaged $\bar{n}(z)$ and macroscopically averaged $\bar{\bar{n}}(z)$ electronic charge densities are shown in solid and dotted lines respectively. The horizontal line indicating the level of 8 electrons per unit cell as the mean value of the two latter curves. (d) The total (electronic plus ionic) double macroscopic average of the electrostatic potential.

Figure 3: Total electrostatic potential lineups, in the $(GaAs)_3/(InAs)_3$ (001) supercell, versus strain effects (in-plane lattice constants), as applied by various substrates. All the curves are scaled in the z-direction to adapt the length of supercell 2.

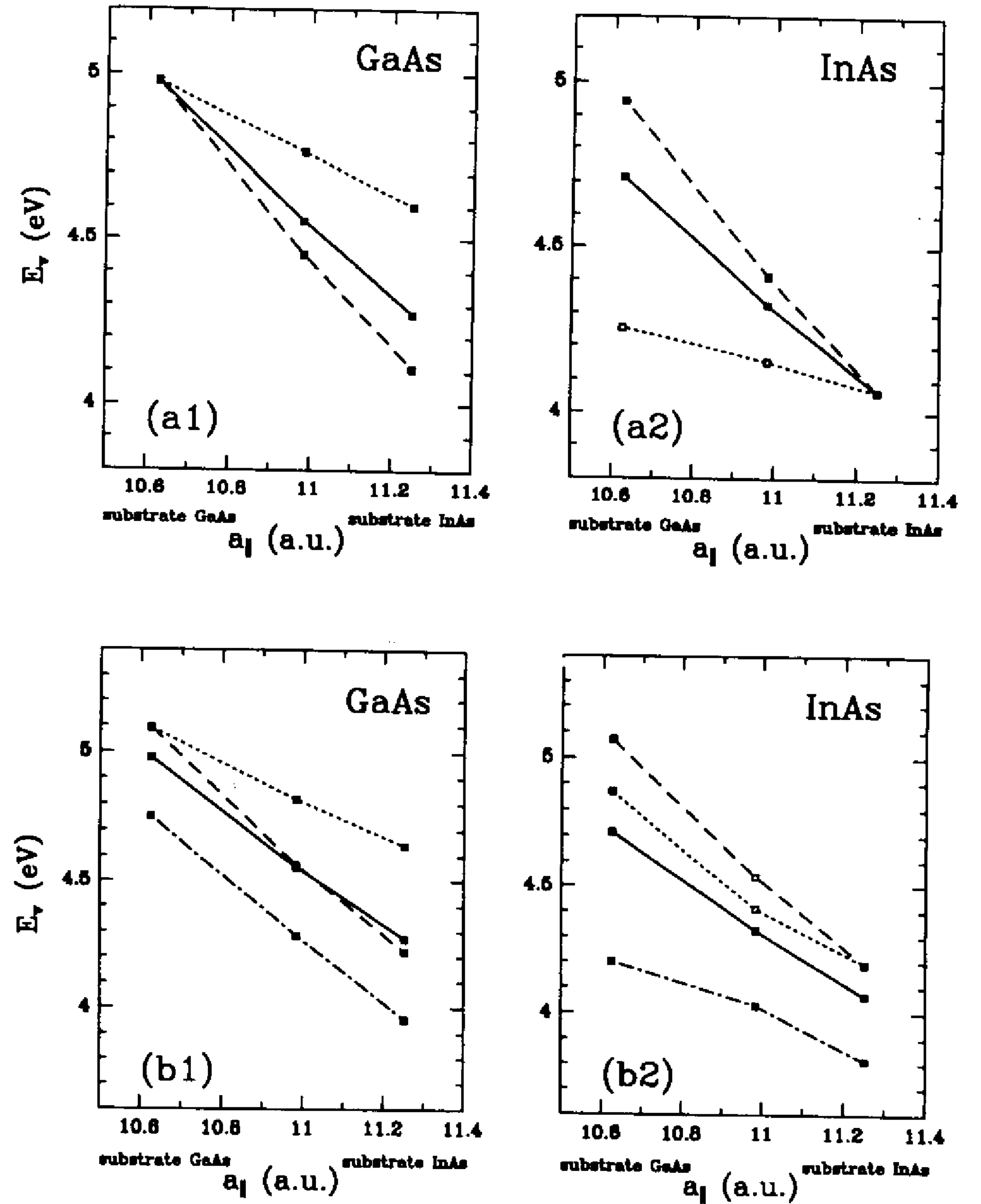

Fig.1

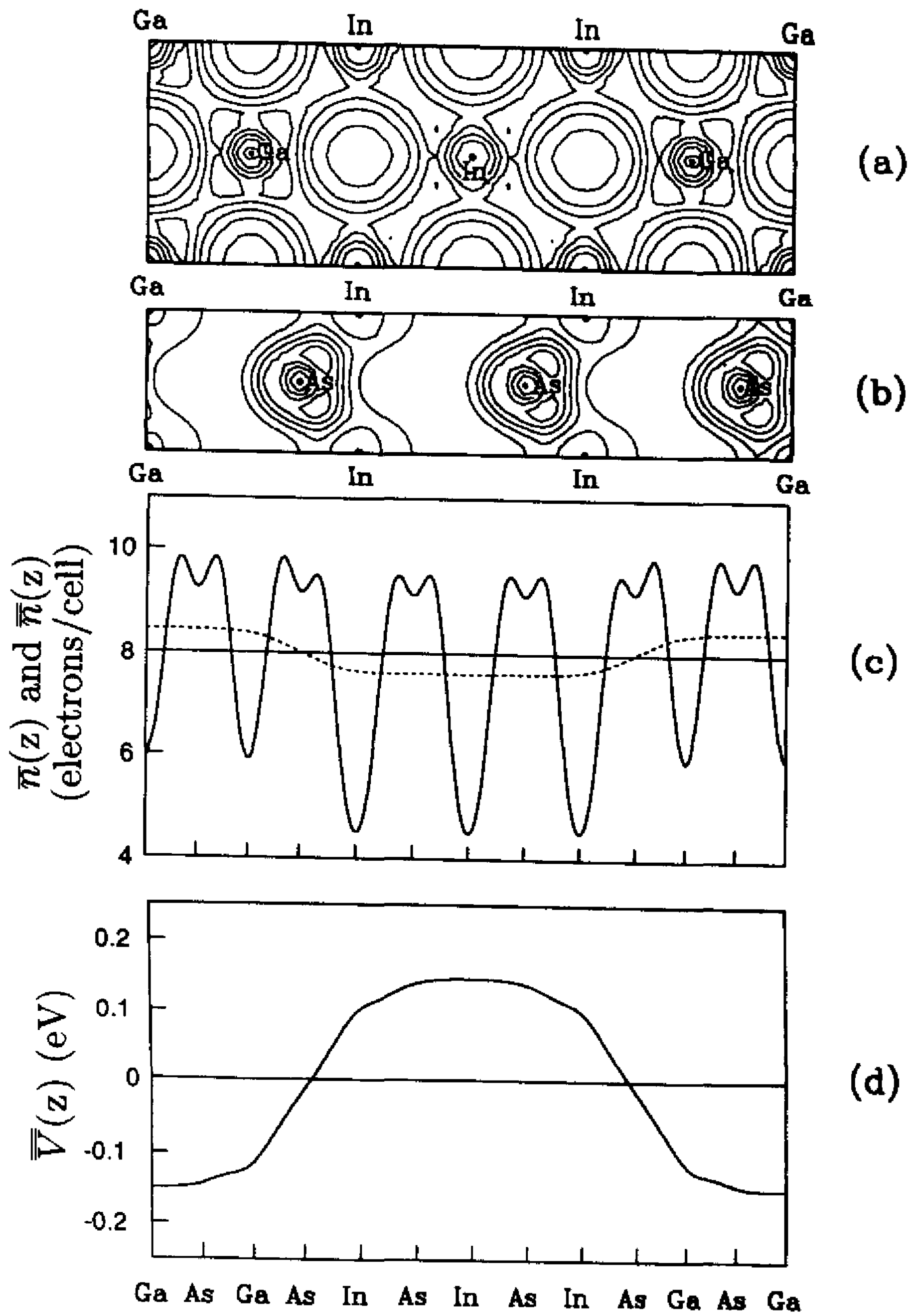

Fig.2

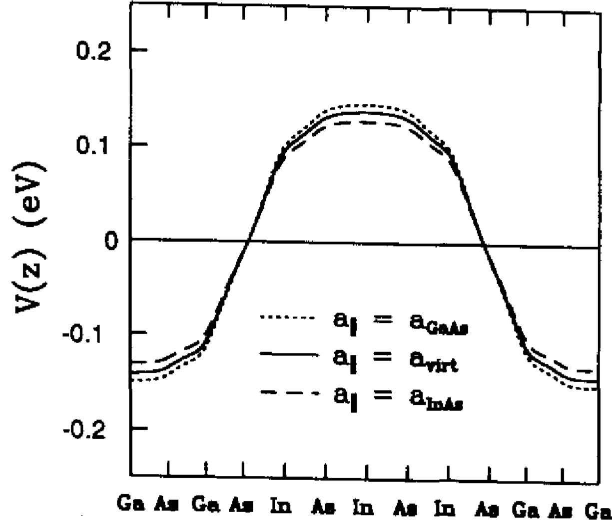

Fig.3